Inorg. Chem. **2003**, *42*, 5507–5512

Synthesis and Magnetic Properties of Heterometal Cyclic Tetranuclear Complexes $[Cu^{II}LM^{II}(hfac)]_2$ (M^{II} = Zn, Cu, Ni, Co, Fe, Mn; H_3L = 1-(2-Hydroxybenzamido)-2-((2-hydroxy-3-methoxybenzylidene)amino)ethane; Hhfac = Hexafluoroacetylacetone)

Shutaro Osa,[†] Yukinari Sunatsuki,[‡] Yoko Yamamoto,[†] Masaaki Nakamura,[†] Tomoshige Shimamoto,[†] Naohide Matsumoto,*[,†] and Nazzareno Re[§]

Department of Chemistry and Department of Physics, Faculty of Science, Kumamoto University, Kurokami 2-39-1, Kumamoto 860-8555, Japan, Department of Chemistry, Faculty of Science, Okayama University, Tsushima-naka 3-1-1, Okayama 700-8530, Japan, and Facolta di Farmacia, Università degli Studi "G. D'Annunzio", Chieti, Italy

Received April 15, 2003

A series of heterometal cyclic tetranuclear complexes $[Cu^{II}LM^{II}(hfac)]_2$ (M^{II} = Zn (**1**), Cu (**2**), Ni (**3**), Co (**4**), Fe(**5**), and Mn (**6**)) have been synthesized by the assembly reaction of K[CuL] and $[M^{II}(hfac)_2(H_2O)_2]$ with a 1:1 mole ratio in methanol, where H_3L = 1-(2-hydroxybenzamido)-2-((2-hydroxy-3-methoxybenzylidene)amino)ethane and Hhfac = hexafluoroacetylacetone. The crystal structures of **2**, **4**, and $[Cu^{II}LMn^{II}(acac)]_2$ (**6a**) (Hacac = acetylacetone) were determined by single-crystal X-ray analyses. Each complex has a cyclic tetranuclear $Cu^{II}_2M^{II}_2$ structure, in which the Cu^{II} complex functions as a "*bridging ligand complex*", and the Cu^{II} and M^{II} ions are alternately arrayed. One side of the planar Cu^{II} complex coordinates to one M^{II} ion at the two phenoxo and the methoxy oxygen atoms, and the opposite side of the Cu^{II} complex coordinates to another M^{II} ion at the amido oxygen atom. The temperature-dependent magnetic susceptibilities revealed spin states of S_M = 0, 1/2, 1, 3/2, 2, and 5/2 for the Zn^{II}, Cu^{II}, Ni^{II}, Co^{II}, Fe^{II}, and Mn^{II} ions, respectively. Satisfactory fittings to the observed magnetic susceptibility data were obtained by assuming a rectangular arrangement with two different *g*-factors for the Cu^{II} and M^{II} ions, two different isotropic magnetic exchange interactions, J_1 and J_2, between the Cu^{II} and M^{II} ions, and a zero-field splitting term for the M^{II} ion. In all cases, the antiferromagnetic coupling constants were found for both exchange interactions suggesting nonzero spin ground states with $S_T = 2|S_M - S_{Cu}|$, which were confirmed by the analysis of the field-dependent magnetization measurements.

Introduction

Magnetochemistry on heterometal polynuclear complexes has attracted much attention for a long time both from the material science and model study of metal enzymes. The molecular-based magnetic materials have shown spectacular advances over the last two decades,[1] in which the study of heterometal binuclear complexes has played an important and leading role. A number of heterometal binuclear complexes have been synthesized and their magnetic properties have been investingated.[2] Kahn introduced the concept of magnetic orthogonality and succeeded in predicting the magnetic interaction between the magnetic centers with the various magnetic orbitals.[3] At present, one can predict the magnetic interaction for a given binuclear complex on the basis of the electronic structures of the magnetic orbitals and the bridging geometry. Furthermore, this information can be successfully applied to the synthesis of multidimensional

* To whom correspondence should be addressed. E-mail: naohide@aster.sci.kumamoto-u.ac.jp. Fax: +81-96-342-3390.
[†] Kumamoto University.
[‡] Okayama University.
[§] Università degli Studi "G. D'Annunzio".

(1) (a) *Magnetic Molecular Materials*; Gatteschi, D., Kahn, O., Miller, J. S., Palacio, F., Eds.; NATO ASI Series E, Vol. 198; Kluwer Academic Publishers: Dordrecht, The Netherlands, 1991. (b) *Magnetism: A Supramolecular Function*; Kahn, O., Ed.; NATO ASI Series C, Vol. 484; Kluwer Academic Publishers: Dordrecht, The Netherlands, 1996.

(2) (a) Journaux, Y.; Kahn, O.; Zarembowitch, J.; Galy, J.; Jaud, J. *J. Am. Chem. Soc.* **1983**, *105*, 7585−7591. (b) Kahn, O.; Galy, J.; Journaux, Y.; Moregenstern-Badarau, I. *J. Am. Chem. Soc.* **1982**, *104*, 2165−2176. (c) Morgenstern-Badarau, I.; Rerat, M.; Kahn, O.; Jaud, J.; Galy, J. *Inorg. Chem.* **1982**, *21*, 3050−3059. (d) Ohba, M.; Tamaki, H.; Matsumoto, N.; Okawa, H. *Inorg. Chem.* **1993**, *32*, 5385−5390.

(3) Kahn, O. *Molecular Magnetism*; VCH: Weinheim, Germany, 1993.

10.1021/ic0344012 CCC: $25.00
Published on Web 08/06/2003

Chart 1. Heterometal Cyclic Tetranuclear Complexes $[Cu^{II}LM^{II}(hfac)]_2$ (M^{II} = Zn^{II}, Cu^{II}, Ni^{II}, Co^{II}, and Mn^{II}) and Their Spin Arrangements

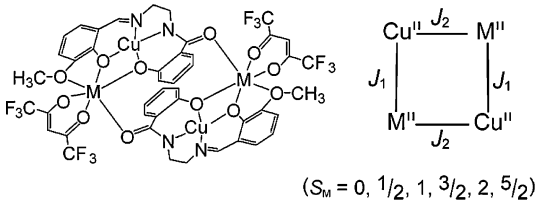

magnetic materials exhibiting magnetic ordering and spontaneous magnetization.[4] A number of versatile molecular-based magnetic materials have been designed and synthesized from the molecular level. However, the combinations of the heterometal ions so far investigated are still far from all possible combinations, and the versatilities of the nuclearlities and arrangement of the constituting metal ions are still limited to several examples. Thus, the magnetochemistry of heterometal polynuclear complexes is increasing its importance.

A heterometal cyclic tetranuclear complex can be a good probe to evaluate the magnetic interaction, because there are at least two intramolcular magnetic interactions and these two magnetic interactions compete to produce the magnetic property of the compounds. If these two magnetic interactions were both antiferromagnetic, the spin ground state of the molecule will be $S_T = 2|S_1 - S_2|$. If one magnetic interaction was ferromagnetic while the other was antiferromagnetic, the spin ground state of the molecule will be zero.[5] If two magnetic interactions were both ferromagnetic, a high-spin molecule with the spin ground state of $S_T = 2|S_1 + S_2|$ can be generated.[6] From this viewpoint, a series of heterometal cyclic tetranuclear complexes $[Cu^{II}LM^{II}(hfac)]_2$ (M^{II} = Zn (**1**), Cu (**2**), Ni (**3**), Co (**4**), Fe(**5**), and Mn (**6**)) have been synthesized and their magnetic properties were investigated (see Chart 1).

Results and Discussion

Synthesis and Characterization of Heterometal Cyclic Tetranuclear Complexes $[Cu^{II}LM^{II}(hfac)]_2$ (M^{II} = Zn (1), Cu (2), Ni (3), Co (4), Fe(5), and Mn (6)). A series of heterometal cyclic tetranuclear complexes was synthesized by the assembly reaction of $K[Cu^{II}L]$ and $[M^{II}(hfac)_2(H_2O)_2]$, in which $K[Cu^{II}L]$ that functions as a "*bridging ligand complex*" is a donor component during the formation of coordination bonds and $[M^{II}(hfac)_2(H_2O)_2]$ is an acceptor component exhibiting substitutable coordination sites. The phenoxo and methoxy oxygen atoms of the Cu^{II} component coordinate to one M^{II} ion, and the amide oxygen atom at the opposite side further coordinates to another M^{II} ion. The hexafluoroacetylacetonato moiety ($hfac^-$) of $[M^{II}(hfac)_2(H_2O)_2]$ can be easily substituted by the ligand with stronger external donor atoms and can also function as a mononegative capping or terminal ligand.

The mixing of methanolic solutions of $K[Cu^{II}L]$ and $[M^{II}(hfac)_2(H_2O)_2]$ (M^{II} = Zn, Cu, Ni, Co, and Mn) at the 1:1 mole ratio gave heterometal complexes with the chemical formula $[Cu^{II}LM^{II}(hfac)]_2$, where 1 $hfac^-$ ligand/M^{II} ion is eliminated during the reaction to give an electrically neutral species, $[Cu^{II}LM^{II}(hfac)]_2$. Each infrared spectrum exhibits an intense absorption band assignable to the $\nu_{C=O}$ vibration of the amido moiety at 1646−1654 cm^{-1},[7] whose wavenumber is shifted to a higher wavenumber from 1644 cm^{-1} for the component complex $K[CuL]$.[8]

Table 1. X-ray Crystallographic Data for $[CuLCu(hfac)]_2$ (**2**), $[CuLCo(hfac)]_2$ (**4**), and $[CuLMn(acac)]_2$ (**6a**)[a]

param	2	4	6a
formula	$C_{22.5}H_{17}N_2O_6F_6ClCu_2$	$C_{22.5}H_{17}N_2O_6F_6ClCoCu$	$C_{22}H_{22}N_2O_6MnCu$
fw	687.93	683.32	528.90
space group	$P2_1/n$ (No. 14)	$P2_1/n$ (No. 14)	$P\bar{1}$ (No. 2)
a, Å	17.488(6)	17.49(2)	9.522(5)
b, Å	10.551(8)	10.549(8)	11.491(3)
c, Å	15.329(4)	15.63(1)	12.098(3)
α, deg	90	90	94.90(2)
β, deg	108.71(2)	110.15(7)	111.34(3)
γ, deg	90	90	113.13(3)
V, Å^3	2679.0(2)	2706.8(4)	1092.8(1)
Z	4	4	2
$D_{calc.}$, g cm^{-3}	1.705	1.677	1.607
μ, cm^{-1}	17.69	15.78	15.92
R, R_w	0.064, 0.062	0.057, 0.180	0.035, 0.039

[a] The crystals of **2** and **4** contain a dichloromethane molecule as the crystal solvent.

Structural Description of $[Cu^{II}LM^{II}(hfac)]_2$ (M^{II} = Cu-(2), Co(4)) and $[Cu^{II}LMn^{II}(acac)]_2$ (6a). The crystal structures were determined by single-crystal X-ray diffraction analyses. Their crystallographic data are summarized in Table 1. Selected bond distances with their estimated standard deviations in parentheses are given in Table 2. These structures are very similar to those of the previously reported Cu^{II}_2-Ln^{III}_2 complexes.[6] As these molecular structures are similar to each other, only the structure of **6a** is described in detail. Figure 1 shows a cyclic $Cu^{II}_2Mn^{II}_2$ tetranuclear structure of **6a** with the atom numbering scheme, in which the molecule has an inversion center and the Cu^{II} and Mn^{II} ions are alternately arrayed. The Cu^{II} ion has a square planar coordination geometry with the N_2O_2 donor atoms of the nonequivalent tetradentate ligand L^{3-}. The Cu−N and Cu−O distances of the 2-oxybenzamido moiety (Cu−N(1) = 1.890(3) Å, Cu−

(4) (a) Kahn, O.; Pei, Y.; Verdaguer, M.; Renard, J. P.; Sletten, J. *J. Am. Chem. Soc.* **1988**, *110*, 782−789. (b) Miller, J. S.; Calabrese, J. C.; Rommelmann, H.; Chittipeddi, S. R.; Zhang, J. H.; Reiff, W. M.; Epstein, A. J. *J. Am. Chem. Soc.* **1987**, *109*, 769−781. (c) Caneschi, A.; Gatteschi, D.; Sessoli, R. *Acc. Chem. Res.* **1989**, *22*, 393−398. (d) Tamaki, H.; Zhong, Z.; Matsumoto, N.; Kida, S.; Koikawa, M.; Achiwa, N.; Hashimoto, Y.; Okawa, H. *J. Am. Chem. Soc.* **1992**, *114*, 6974−6979. (e) Miyasaka, H.; Matsumoto, N.; Okawa, H.; Re, N.; Gallo, E.; Floriani, *J. Am. Chem. Soc.* **1996**, *118*, 981−994.

(5) (a) Ribas, J.; Diaz, C.; Costa, R.; Tercero, J.; Solans, X.; Font-Bardia, M.; Stoeckli-Evans, H. *Inorg. Chem.* **1998**, *37*, 233−239. (b) Tercero, J.; Diaz, C.; Ribas, J.; Ruiz, E.; Mahia, J.; Maestro, M. *Inorg. Chem.* **2002**, *47*, 6780−6789.

(6) (a) Kido, T.; Nagasato, S.; Sunatsuki, Y.; Matsumoto, N. *Chem. Commun.* **2000**, 2113-2114. (b) Kido, T.; Ikta, Y.; Sunatsuki, Y.; Ogawa, Y.; Matsumoto, N.; Re, N. *Inorg. Chem.* **2003**, *42*, 398−408. (c) Costes, J.-P.; Dahan, F. *C. R. Acad. Sci., Ser. 2c* **2001**, *4*, 97−103.

(7) Nakamoto, K. In *Infrared and Raman Spectra of Inorganic and Coordination Compounds*, 5th ed.; John Wiley and Sons: New York, 1997; Part B, Chapter III-14.

(8) Sunatsuki, Y.; Matsuo, T.; Nakamura, M.; Kai, F.; Matsumoto, N.; Tuchagues, J.-P. *Bull. Chem. Soc. Jpn.* **1998**, *71*, 2611−2619.

Table 2. Relevant Distances (Å) for [CuLCu(hfac)]$_2$ (**2**), [CuLCo(hfac)]$_2$ (**4**), and [CuLMn(acac)]$_2$ (**6a**)

[CuLCu(hfac)]$_2$ (**2**)		[CuLCo(hfac)]$_2$ (**4**)		[CuLMn(acac)]$_2$ (**6a**)	
Cu(1)···Cu(1)^a	4.528(4)	Cu···Cu^a	4.670(4)	Cu···Cu^a	4.853(3)
Cu(2)···Cu(2)^a	7.201(3)	Co···Co^a	7.096(4)	Mn···Mn^a	7.303(2)
Cu(1)···Cu(2)	3.132(2)	Cu···Co	3.072(3)	Cu···Mn	3.183(2)
Cu(1)···Cu(2)^a	5.135(3)	Cu···Co^a	5.162(3)	Cu···Mn^a	5.321(3)
Cu(1)−N(1)	1.915(6)	Cu−N(1)	1.896(5)	Cu−N(1)	1.890(3)
Cu(1)−N(2)	1.906(6)	Cu−N(2)	1.927(5)	Cu−N(2)	1.928(4)
Cu(1)−O(2)	1.883(5)	Cu−O(2)	1.895(4)	Cu−O(2)	1.898(3)
Cu(1)−O(3)	1.941(5)	Cu−O(3)	1.910(4)	Cu−O(3)	1.906(3)
Cu(2)^a−O(1)	1.947(5)	Co^a−O(1)	1.994(4)	Mn^a−O(1)	2.102(3)
Cu(2)−O(2)	2.376(5)	Co−O(2)	2.196(4)	Mn−O(2)	2.247(3)
Cu(2)−O(3)	1.976(5)	Co−O(3)	2.009(4)	Mn−O(3)	2.150(3)
Cu(2)−O(4)	2.342(5)	Co−O(4)	2.282(4)	Mn−O(4)	2.470(3)
Cu(2)−O(5)	1.954(5)	Co−O(5)	2.062(5)	Mn−O(5)	2.103(3)
Cu(2)−O(6)	1.952(6)	Co−O(6)	2.019(5)	Mn−O(6)	2.100(3)

^{a} Denotes the symmetry operation of $-x, -y, -z$.

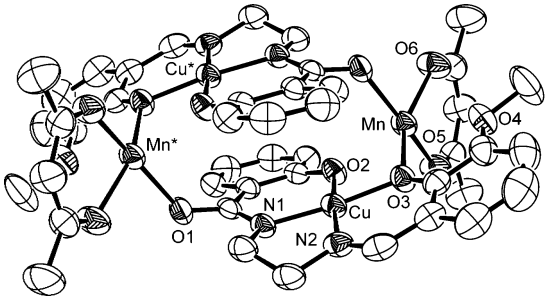

Figure 1. Molecular structure of cyclic tetranuclear complex [Cu^{II}LMn^{II}-(acac)]$_2$ (**6a**) with the selected atom labeling scheme. The hydrogen atoms are omitted for clarity.

O(2) = 1.898(3) Å) are considerably shorter than the corresponding values of the 2-oxy-3-methoxybenzaldehyde moiety (Cu−N(2) = 1.928(4) Å, Cu−O(3) = 1.906(3) Å). In the cyclic structure, the Cu^{II} complex functions as an electrically mononegative "bridging ligand complex" between the two M^{II} ions. The two phenoxo (O(2) and O(3)) and the methoxy (O(4)) atoms on one side of the planar Cu^{II} complex coordinate to a M^{II} ion as a tridentate ligand with distances of Mn−O(2) = 2.247(3) Å, Mn−O(3) = 2.150(3) Å, Mn−O(4) = 2.470(3) Å, and Cu(1)···Mn = 3.183(2) Å. The amido oxygen atom (O(1)) on the opposite side of the Cu^{II} complex coordinates to another Mn^{II} ion as a monodentate ligand with the distance of Mn*−O(1) = 2.102(3) Å and Cu···Mn* = 5.321(3) Å. Including the coordination of a acac$^-$ ion as a bidentate chelate ligand (Mn−O(5) = 2.103(3), Mn−O(6) = 2.100(3) Å), the Mn^{II} ion has a hexacoordinate geometry with the O_6 oxygen atoms. It should be noted that the Mn−O bond distance with the amido oxygen is the shortest among the six Mn−O bonds. In a cyclic structure, there is no bridging ligand between the two Cu^{II} ions and between the two Mn^{II} ions, where the distances of Cu···Cu* and Mn···Mn* are 4.853(3) and 7.303(2) Å, respectively.

Magnetic Properties of [Cu^{II}LM^{II}(hfac)]$_2$ (1−6). The magnetic susceptibilities were measured under an external applied magnetic field of 1 T in the temperature range 2−300 K. The magnetic behaviors are shown in Figure 2, as the plots of $\chi_M T$/tetranuclear molecule vs T. The $\chi_M T$ values of **1**−**6** at room temperature demonstrated that the spin states of the M^{II} ions are S_M = 0, 1/2, 1, 3/2, 2, and 5/2 for Zn^{II}, Cu^{II}, Ni^{II}, Co^{II}, Fe^{II}, and Mn^{II}, respectively. The $\chi_M T$ value of [Cu^{II}LZn^{II}(hfac)]$_2$ (**1**) is practically constant over the entire temperature range, indicating that the intra- and intermolecular Cu−Cu magnetic interactions are small. Upon lowering of the temperature, the $\chi_M T$ values of **2**−**4** monotonically decrease. On the other hand, the $\chi_M T$ values of **5** and **6** first decrease and reach a minimum, then increase to a maximum, and finally decrease at low temperatures. To reproduce these magnetic susceptibility data and to evaluate the magnetic interaction parameters, we used the following spin-only Hamiltonian based on a cyclic tetranuclear structure with a rectangular arrangement:

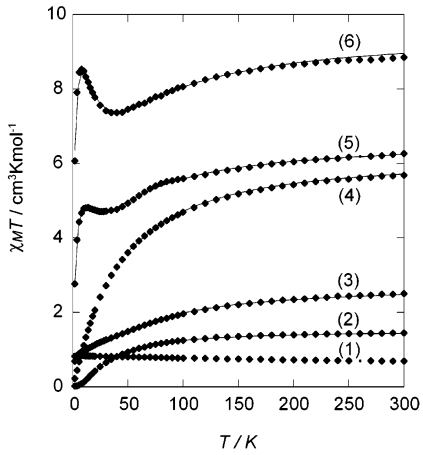

Figure 2. Plots of $\chi_M T$ vs temperature for heterometal cyclic tetranuclear complexes [Cu^{II}LM^{II}(hfac)]$_2$ ((M^{II} = Zn (**1**), Cu (**2**), Ni (**3**), Co (**4**), Fe (**5**), and Mn (**6**)). The solid lines represent the theoretical curves with the fitting parameters given in the text.

$$\mathbf{H} = g_{Cu}\beta(\boldsymbol{S_1} + \boldsymbol{S_3})\cdot H + g_M\beta(\boldsymbol{S_2} + \boldsymbol{S_4})\cdot H + 2J_1(\boldsymbol{S_1}\cdot\boldsymbol{S_2} + \boldsymbol{S_3}\cdot\boldsymbol{S_4}) + 2J_2(\boldsymbol{S_2}\cdot\boldsymbol{S_3} + \boldsymbol{S_4}\cdot\boldsymbol{S_1}) + D[\mathbf{S_{2z}}^2 - S_M(S_M + 1)] + D[\mathbf{S_{4z}}^2 - S_M(S_M + 1)] \quad (1)$$

Here H is the applied field, J_1 and J_2 are the Heisenberg coupling constants for the two different magnetic paths shown in Chart 1, g_{Cu} and g_M are the g-factors for the Cu^{II} and M^{II} ions, respectively, and D is the zero-field splitting parameter for the M^{II} ions. The intramolecular Cu^{II}−Cu^{II} and M^{II}−M^{II} magnetic interactions have been both neglected, because no Cu^{II}−Cu^{II} magnetic interaction was detected in [Cu^{II}LZn^{II}(hfac)]$_2$ (**1**) and the M^{II}−M^{II} distance is longer than the Cu^{II}−Cu^{II} one (see above) suggesting also no M^{II}−M^{II} magnetic interaction. The magnetic susceptibility at each temperature was calculated by using the theoretical equation

$$M = [N\Sigma_i(-dE_i/dH)\exp(-E_i/kT)]/[\Sigma_i\exp(-E_i/kT)] \quad (2)$$

and $\chi = M/H$. The energy levels of the tetramer, E_i, were evaluated by diagonalizing the Hamiltonian matrix in the uncoupled spin function basis set. Moreover, a molecular field term $-zJ'\langle S_z\rangle S_z$ was added to the Hamiltonian to describe the molecular interactions between the tetrameric units. Although small, these interactions are necessary to reproduce the decrease in the magnetic moment below 4 K.

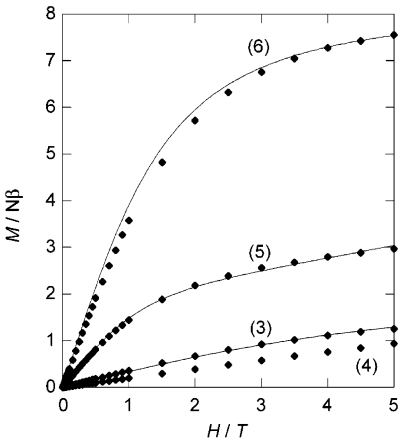

Figure 3. Field dependence of the magnetization of $[Cu^{II}LM^{II}(hfac)]_2$ ((M^{II} = Ni (**3**), Co (**4**), Fe(**5**), and Mn (**6**)) at 4 K. The solid lines represent the theoretical curves with the fitting parameters given in the text.

The final expression for the magnetic susceptibility becomes[3]

$$\chi_{mf} = \chi/[1 - zJ'\chi/Ng^2\beta^2] \quad (3)$$

where χ is the magnetic susceptibility for the isolated tetramer calculated as described above.

The magnetic susceptibility data of all the complexes were well reproduced over the entire temperature range, except for $[Cu^{II}LCo^{II}(hfac)]_2$ (**4**), for which we were limited to the 50−300 K range, and the theoretical curves are shown as the solid lines in Figure 2. The calculated fitting parameters were $g_{Cu} = 2.02$, $J_1 = -13.3$ cm^{-1}, and $J_2 = -13.3$ cm^{-1} for $[Cu^{II}LCu^{II}(hfac)]_2$ (**2**); $g_{Cu} = 1.92$, $g_{Ni} = 2.03$, $J_1 = -15.8$ cm^{-1}, $J_2 = -15.8$ cm^{-1}, and $D_{Ni} = +6.9$ cm^{-1} for $[Cu^{II}LNi^{II}(hfac)]_2$ (**3**); $g_{Cu} = 1.97$, $g_{Fe} = 1.98$, $J_1 = -10.9$ cm^{-1}, $J_2 = -3.7$ cm^{-1}, $D_{Fe} = -1.6$ cm^{-1}, and $zJ' = -0.09$ cm^{-1} for $[Cu^{II}LFe^{II}(hfac)]_2$ (**5**); and $g_{Cu} = 1.98$, $g_{Mn} = 2.02$, $J_1 = -11.0$ cm^{-1}, $J_2 = -3.8$ cm^{-1}, and $zJ' = -0.06$ cm^{-1} for $[Cu^{II}LMn^{II}(hfac)]_2$ (**6**). The interpretation of the magnetic properties of $[Cu^{II}LCo^{II}(hfac)]_2$ (**4**) is complicated due to the unquenched orbital momentum of the Co^{II} ion. The isotropic Heisenberg exchange model is not strictly applicable to octahedral Co^{II} complexes because of the strong spin−orbit splitting of the $^4T_{1g}$ (F) ground term but can be applied to distorted octahedral geometries where the orbital degeneracy of the $^4T_{1g}$ state is removed. However, at low temperatures, the states arising from the $^4T_{1g}$ term are split into two Kramer doublets by spin−orbit coupling and the Heisenberg model may fail. The magnetic data for **4** could not be satisfactorily fitted over the entire temperature range using the Hamiltonian in eq 1 in which the quartet state splitting is accounted for by the axial single-ion zero field interaction $D(\mathbf{S}_z^2 - 15/2)$. However, a reasonable fit could be performed in the 50−300 K region neglecting the zero-field interaction and lead to $g_{Co} = 2.37$, $g_{Cu} = 2.25$, $J_1 = -20.2$ cm^{-1}, and $J_2 = -0.3$ cm^{-1}.

The field dependence of the magnetization for **3**−**6** were measured up to 5 T at 4 K to determine their spin ground states and anisotropic properties. Figure 3 shows the experimental results as the plots of $M/N\beta$ vs H at 4 K. The variation in the magnetization with H/T for a molecule with an isolated spin multiplet S as the ground state is described by the Brillouin function, i.e., by expression (4),

$$M/N\beta = gS[B_S(z)] \quad (4)$$

where $z = g\beta H/kT$ and $B_S(z)$ is the Brillouin function for the S state.[9] The magnetization data of **6** is well reproduced by the Brillouin function (4) for $S = 4$ and $g = 1.97$ (the solid line). Therefore, the curve fitting of the magnetization as well as that of the magnetic susceptibility data clearly showed that compound **6** has an $S = 4$ spin ground state resulting from two antiferromagnetic interactions in the cyclic (1/2, 5/2, 1/2, 5/2) spin system. The magnetization curve of **3** is lower than the theoretical curve calculated from eq 4 (the solid line) for an $S = 1$ ground state resulting from the antiferromagnetic interactions in the cyclic (1/2, 1, 1/2, 1) spin system. It must be considered that, due to the relevant zero field splitting, the $S = 1$ ground state is split into two $M_S = 0$ and ± 1 components, thus leading to a deviation from the Brillouin behavior.[10] The correct dependence of the theoretical magnetization as a function of the field H can be obtained through the full-matrix diagonalization of the Hamiltonian matrix, using the three spin functions of the $S = 1$ state and the Hamiltonian

$$\mathbf{H} = g_S\beta S\cdot H + D[\mathbf{S}_z^2 - S(S+1)] \quad (5)$$

The obtained eigenvalues E_i and their derivatives with respect to the magnetic field were used to calculate the magnetization using eq 2. The best fit of the magnetization data of **3** was obtained for $g = 2.00$, and $D = +5.2$ cm^{-1} as shown by the solid line in Figure 3. Note that these values agree quite well with those obtained from the variable-temperature magnetic susceptibility fitting ($g_{av} = 1.98$, $D = +6.9$ cm^{-1}), the small observed differences being probably due to the neglected effects of rhombic anisotropy or to the presence of low-lying excited spin states. This agreement between the parameters obtained in the $\chi_M T$ vs T and $M/N\beta$ vs H fittings confirms both the goodness of our spin coupling model and the $S = 1$ nature of the ground state of compound **3**. The magnetization data for complex **5** are much lower than those expected from the Brillouin function (4). The magnetization seems to saturate at a value of about 3.0, which is much less than the value of 6.0, expected by eq 4 for the $S = 3$ ground state resulting from the antiferromagnetic interactions in the cyclic (1/2, 2, 1/2, 2) spin system. This is due to the zero-field splitting interactions which split the $S = 3$ ground state into four $M_S = 0$, ± 1, ± 2, and ± 3 components.[10] The correct dependence of the magnetization as a function of the field H has been obtained through the full-matrix diagonalization of the Hamiltonian matrix, built with the seven spin functions of the $S = 3$ state and the Hamiltonian (5) and introducing the eigenvalues in eq 2. The experimental data are well reproduced by the parameters of $g = 1.93$ and $D = -2.2$ cm^{-1}. The sign of the zero-field

(9) Carlin, R. L. *Magnetochemistry*; Springer-Verlag: Berlin, 1986.
(10) Vincent, J. B.; Christmas, C.; Chang, H. R.; Li, Q.; Boyd, P. D. W.; Huffman, J. C.; Hendrickson, D. N.; Cristou, G. *J. Am. Chem. Soc.* **1989**, *111*, 2086−2097.

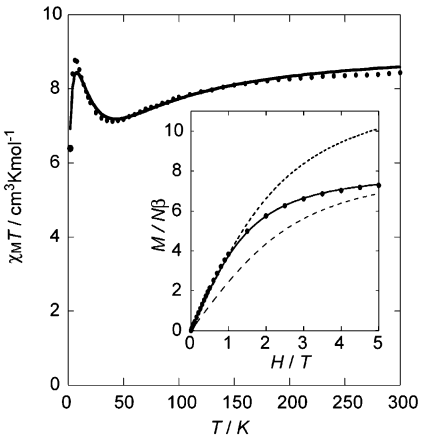

Figure 4. Plots of $\chi_M T$ vs T and $M/N\beta$ vs H at 4 K (inset) of $[Cu^{II}LMn^{II}(acac)]_2$ (**6a**). The solid curve in the $\chi_M T$ vs T plot represents the theoretical curve with the parameters of $g_{Cu} = 1.98$, $g_{Mn} = 1.97$, $J_1 = -11.0$ cm^{-1}, $J_2 = -3.9$ cm^{-1}, and $zJ' = -0.04$ cm^{-1}. The $M/N\beta$ curve is larger than the Brillouin functions for two independent $S = 2$ spins (dashed curve) and smaller than those for a magnetically isolated (1/2, 5/2, 1/2, 5/2) system (dotted curve). The experimental data are well reproduced by the Brillouin function with $S = 4$ and $g = 2.00$ (solid curve).

splitting parameter D cannot be unequivocally determined by the magnetic susceptibility analysis but may be obtained by low-temperature saturation magnetization data which are differently fitted by positive or negative values of D. Indeed, for negative D values the saturation magnetization curve of a high-spin isolated ground-state S evidences a change in slope due to the quick saturation of the $M = \pm S$ lower states at low fields, leading to a steeper slope which is reduced at higher fields as the highest $M = 0$ state is saturated. In the case of complex **5** a change in slope is evidenced at ca. 2 T; see Figure 3. Large zero-field splitting parameters are quite common for Fe^{II} complexes due to the orbital degeneracy of their ground states.[9] Although positive D values are usually observed, negative values have been reported for distorted octahedral complexes on the basis of magnetization data and Mössbauer spectroscopy.[11] The value of the zero-field splitting parameter determined by the magnetization data ($D = -2.2$ cm^{-1}) is consistent with the value obtained from the magnetic susceptibility analysis ($D = -1.6$ cm^{-1}), thus confirming that compound **5** has an $S = 3$ spin ground state. For $[Cu^{II}LCo^{II}(hfac)]_2$ (**4**), the $M/N\beta$ vs H plot saturates at a very low value, much smaller than that expected from the Brillouin function for an $S = 2$ state as a result of the antiferromagnetic coupling in the cyclic (1/2, 3/2, 1/2, 3/2) spin system. The strong spin−orbit coupling due to the unquenched orbital momentum and the presence of several low-lying spin states makes its fitting with an isolated spin-state model impossible.

Figure 4 shows the $\chi_M T$ vs T plots and the $M/N\beta$ vs H plots (inset) of **6a**. The $\chi_M T$ curve was well reproduced by the parameters of $g_{Cu} = 1.98$, $g_{Mn} = 1.97$, $J_1 = -11.0$ cm^{-1}, $J_2 = -3.9$ cm^{-1}, and $zJ' = -0.04$ cm^{-1}. The $M/N\beta$ curve is larger than the Brillouin functions for two independent $S = 2$ spins (dashed curve) and smaller than those for a magnetically isolated (1/2, 5/2, 1/2, 5/2) system (dotted curve). The experimental data are well reproduced by the Brillouin function with $S = 4$ and $g = 2.00$ (solid curve).

Qualitative Consideration for the Nature of the Magnetic Interaction. A qualitative rationale for the trend and the nature of the exchange interactions between the Cu^{II} and M^{II} ions can be provided on the basis of a simple metal orbital picture.[3] The sign of the intramolecular exchange coupling constants is determined by the sum of antiferromagnetic and ferromagnetic contributions, $J = J_{AF} + J_F$. The environment around the d^9 Cu^{II} ion is a square planar, and thus the magnetic orbital is $d_{x^2-y^2}$ pointing from the metal toward the four donor atoms (N_2O_2) and overlaps on either side of the bridging phenoxo ligands or N−C−O unit with the magnetic orbitals of the two adjacent M^{II} ions, leading to the J_1 and J_2, respectively. In all considered complexes **2**−**6** the octahedral coordinated M^{II} ion bears at least an e_g magnetic orbital of σ-symmetry pointing toward the six coordinating oxygen atoms, so that the principal magnetic exchange pathway is considered to be of σ nature. Thus, the antiferromagnetic nature of both J_1 and J_2 exchange interactions in **2**−**6** is determined by the symmetry-allowed $d_{x^2-y^2}||p(O)||e_g$ or $d_{x^2-y^2}||p(N)||p(C)||p(O)||e_g$ (using Ginsberg's symbols)[12] σ-superexchange pathways. Moreover, when M^{II} is Cu^{II}, with a $(t_{2g})^6(e_g)^3$ configuration, and Ni^{II}, with a $(t_{2g})^6(e_g)^2$ configuration, only this σ antiferromagnetic contribution is possible, while when M^{II} is hs Co^{II}, $(t_{2g})^5(e_g)^2$, hs Fe^{II}, $(t_{2g})^4(e_g)^2$, and hs Mn^{II}, $(t_{2g})^3(e_g)^2$, orthogonal $d_{x^2-y^2} \perp t_{2g}$ pathways are also allowed and provide ferromagnetic contributions to the overall magnetic interaction, leading to a reduction in the strength of the net antiferromagnetic spin coupling between Cu^{II} and M^{II}. Therefore, the highest antiferromagnetic coupling constants are expected for the $M^{II} = Cu^{II}$ and Ni^{II} as actually observed for both J_1 and J_2 constants with the only exception of the Cu_2Co_2 complex where, however, the high antiferromagnetic J_1 value could be due to the strong spin−orbit coupling within the Co^{II} spin states.

On the basis of the longer −N−C−O− bridge with respect to the phenoxo bridges, the J_2 coupling constant is expected smaller than J_1. This is actually observed for **4**, **5**, **6**, and **6a** but not for the Cu_4 and Cu_2Ni_2 complexes **2** and **3** for which identical J_1 and J_2 values are obtained. However, this may originate from the fact that when the low-temperature increase of the magnetic susceptibility of a rectangular spin arrangement with both antiferromagnetic interactions is not observed due to a singlet ground state as in **2** or to a strong zero-field splitting as in **3**, the magnetic data are not much sensitive to the J_1/J_2 ratio. Indeed trial fittings performed fixing J_2 to a small negative value and optimizing all the remaining parameters leads to higher J_1 values (accounting for the lower J_2) and to discrepancy factors $R = [\Sigma_i(\chi_M T_{obsd} - \chi_M T_{calc})^2/[\Sigma_i(\chi_M T_{obsd})^2]$ only slightly larger than those obtained from the fully free fitting leading to equal J_1 and J_2 values. The physically unfeasible equal values of J_1 and J_2 could be therefore due to such an insensitiveness of the

(11) Clemente-Juan, J. M.; Mackiewicz, C.; Verelst, M.; Dahan, F.; Bousseksou, A.; Sanakis, Y.; Tuchagues, J.-P. *Inorg. Chem.* **2002**, *41*, 1478−1491.

(12) Ginsberg, A. P. *Inorg. Chim. Acta Rev.* **1971**, *5*, 45.

magnetic data to the J_1/J_2 ratio and could be removed through slight corrections of the spin coupling scheme, such as the introduction of cross exchange couplings or rhombic distortions.

Experimental Section

Materials. All chemicals and solvents used for the synthesis were reagent grade and were obtained from Tokyo Kasei Co., Ltd., and used without further purification.

The ligand H_3L and the Cu^{II} complex K[CuL] were prepared according to a previously reported method,[6] where H_3L = 1-(2-hydroxybenzamido)-2-((2-hydroxy-3-methoxybenzylidene)amino)-ethane. $[M^{II}(hfac)_2(H_2O)_2]$ was prepared according to the literature.[13]

[CuLZn(hfac)]$_2$ (1). A methanolic solution (40 mL) of K[CuL] (0.208 g, 0.5 mmol) was gently poured into a methanolic solution (40 mL) of $[Zn(hfac)_2(H_2O)_2]$ (0.258 g, 0.5 mmol) at ambient temperature. The resulting solution was allowed to stand for several days. The violet crystals that formed were collected by filtration and dried under reduced pressure. Yield: 0.378 g (58%). IR (cm^{-1}): $\nu_{C=O}$ 1654; $\nu_{C=N}$ 1602; ν_{CF} 1258−1145. Anal. Calcd for $C_{44}H_{32}N_4O_{12}F_{12}Cu_2Zn_2$: C, 40.82; H, 2.49; N, 4.33. Found: C, 40.62; H, 2.25; N, 4.23.

[CuLCu(hfac)]$_2$ (2). A methanolic solution (30 mL) of K[CuL] (0.208 g, 0.5 mmol) was gently poured into a dichloromethane solution (150 mL) of $[Cu(hfac)_2(H_2O)_2]$ (0.257 g, 0.5 mmol) at ambient temperature. The resulting solution was allowed to stand for several days. Efflorescent brown crystals that formed were collected by filtration, washed with methanol, and dried under reduced pressure. Yield: 0.168 g (26%). IR (cm^{-1}): $\nu_{C=O}$ 1646; $\nu_{C=N}$ 1600; ν_{CF} 1257−1144. Anal. Calcd for $C_{44}H_{32}N_4O_{12}F_{12}Cu_4$: C, 40.94; H, 2.50; N, 4.34. Found: C, 41.30; H, 2.66; N, 4.74.

[CuLNi(hfac)]$_2$ (3). Tetrabutylammonium perchlorate (0.171 g, 0.5 mmol) and K[CuL] (0.208 g, 0.5 mmol) was mixed in a dichloromethane (30 mL) and methanol (10 mL) mixed solution, and the new solution was stirred for 30 min at ambient temperature. The solution was filtered, and the solvent of the filtrate was removed using a rotary evaporator. The residue was dissolved in dichloromethane (30 mL), and the insoluble substance was filtered off. The filtrate was poured into a dichloromethane solution (150 mL) of $[Ni(hfac)_2(H_2O)_2]$ (0.254 g, 0.5 mmol). The resulting solution was allowed to stand for several days. The efflorescent reddish brown crystals that formed were collected by filtration, washed with methanol, and dried under reduced pressure. Yield: 0.126 g (19%). IR (cm^{-1}): $\nu_{C=O}$ 1648; $\nu_{C=N}$ 1600; ν_{CF} 1258−1145. Anal. Calcd for $C_{44}H_{32}N_4O_{12}F_{12}$ $Ni_2Cu_2 \cdot 0.25CH_2Cl_2$: C, 40.81; H, 2.52; N, 4.30. Found: C, 40.87; H, 2.17; N, 4.28.

[CuLCo(hfac)]$_2$ (4). This complex was prepared by the same method as for **2** using $[Co(hfac)_2(H_2O)_2]$ instead of $[Cu(hfac)_2(H_2O)_2]$. Efflorescent brown crystals were obtained. Yield: 0.038 g (6%). IR (cm^{-1}): $\nu_{C=O}$ 1646; $\nu_{C=N}$ 1601; ν_{CF} 1256−1144. Anal. Calcd for $C_{44}H_{32}N_4O_{12}F_{12}Co_2Cu_2$: C, 41.23; H, 2.52; N, 4.37. Found: C, 41.40; H, 2.54; N, 4.39.

[CuLFe(hfac)]$_2$ (5). This complex was prepared by the same method as for **3** using $[Fe(hfac)_2(H_2O)_2]$ instead of $[Ni(hfac)_2(H_2O)_2]$. Dark purple crystals were obtained. Yield: 0.091 g (14%). IR (cm^{-1}): $\nu_{C=O}$ 1646; $\nu_{C=N}$ 1601; ν_{CF} 1257−1144. Anal. Calcd for $C_{44}H_{32}N_4O_{12}F_{12}Fe_2Cu_2 \cdot 0.25CH_2Cl_2$: C, 40.99; H, 2.53; N, 4.32. Found: C, 41.09; H, 2.11; N 4.29.

[CuLMn(hfac)]$_2$ (6). This complex was prepared by the same method as for **2** using $[Mn(hfac)_2(H_2O)_2]$ instead of $[Cu(hfac)_2(H_2O)_2]$. Dark brown crystals were obtained. Yield: 0.154 g (24%). IR (cm^{-1}): $\nu_{C=O}$ 1652; $\nu_{C=N}$ 1601; ν_{CF} 1256−1145. Anal. Calcd for $C_{44}H_{32}N_4O_{12}F_{12}Mn_2Cu_2$: C, 41.49; H, 2.53; N, 4.40. Found: C, 41.25; H, 2.28; N, 4.39.

[CuLMn(acac)]$_2$ (6a). A methanolic solution (20 mL) of K[CuL] (0.208 g, 0.5 mmol) and a methanolic solution (20 mL) of $[Mn(acac)_3]$ (0.176 g, 0.5 mmol) were mixed at ambient temperature. The resulting solution was allowed to stand for several days. The dark red crystals that formed were collected by filtration, washed with methanol, and dried under reduced pressure. Yield: 0.111 g (21%). IR (cm^{-1}): $\nu_{C=O}$ 1654; $\nu_{C=N}$ 1602. Anal. Calcd for $C_{44}H_{44}N_4O_{12}Mn_2Cu_2$: C, 49.96; H, 4.19; N, 5.30. Found: C, 49.62; H, 4.17; N, 4.99.

Physical Measurements. Elemental C, H, and N analyses were carried out at the Center for Instrumental Analysis of Kumamoto University. The infrared spectra were recorded on a Perkin-Elmer FT-IR spectrometer PARAGON 1000 using KBr disks. The temperature-dependent magnetic susceptibilities in the temperature range of 2−300 K under a constant external magnetic field of 1 T and field-dependent magnetization measurements in an applied magnetic field from 0 to 5 T at 2 K were measured with an MPMS-5S SQUID susceptometer (Quantum Design, Inc.). The calibrations were performed with palladium. Corrections for diamagnetism were applied using Pascal's constants.

X-ray Data Collection, Reduction, and Structure Determination. The X-ray data for **2**, **4**, and **6a** were collected on a Rigaku AFC7R diffractometer with graphite monochromated Mo Kα radiation (λ = 0.710 69 Å). The crystals of **2** and **4** contain dichloromethane molecule as the crystal solvent. The dichloromethane is easily eliminated, and the crystal decomposes. The crystal was encapsulated into a glass capillary, and the X-ray diffraction study was performed. An empirical absorption correction was applied. The data were also corrected for Lorentz and polarization effects. The structures were solved by direct methods and expanded using the Fourier technique. The non-hydrogen atoms were anisotropically refined. Hydrogen atoms at their calculated positions were included in the structure factor calculation but were not refined. Full-matrix least-squares refinement based on the observed reflections ($I > 2.00\sigma(I)$) was employed. Neutral atomic scattering factors and anomalous dispersion effects were taken from the literature.[14] All calculations were performed using the CrystalStructure crystallographic software package.[15]

Acknowledgment. This work was supported in part by a Grant-in-Aid for Science Research (No. 14340209) from the Ministry of Education, Science, Sports, and Culture of Japan. Y.S. thanks the Japan Society of Promotion for Science for the postdoctoral fellowship. We are grateful to the JSPS (Japan Society of Promotion for Science) for the bilateral exchange program.

Supporting Information Available: X-ray crystallographic files in CIF format for compounds **2**, **4**, and **6a**. This material is available free of charge via the Internet at http://pubs.acs.org.

IC0344012

(13) Cotton, F. A.; Holm, R. H. *J. Am. Chem. Soc.* **1960**, *82*, 2979−2983.

(14) Cromer, D. T.; Waber, J. T. In *International Tables for X-ray Crystallography*; The Kynoch Press: Birmingham, England, 1974; Vol. IV, Table 2.2A.

(15) *CrystalStructure 2.00 Crystal Structure Analysis Package*; Rigaku and Molecular Structure Corp.: The Woodlands, TX, 2001.